Relative tectonic activity assessment of the Çameli Basin, Western Anatolia, using geomorphic indices

Erman Özsayın

Taylor & Francis
Taylor & Francis Group

Relative tectonic activity assessment of the Çameli Basin, Western Anatolia, using geomorphic indices

Erman Özsayın*

Department of Geological Engineering, Hacettepe University, Ankara TR-06800, Turkey

Western Anatolia is one of the world's most seismically active regions. A nearly N–S-oriented extension caused the formation of E–W- and NE–SW-trending major grabens, creating the potential for earthquakes with magnitudes ≥ 5. The fault segments of the NE-trending Çameli Basin were evaluated using geomorphic indices, common tools for assessment of relative tectonic activity in such areas. Quantitative measurement of geomorphic indices including mountain-front sinuosity (*Smf*; 1.35–2.39), valley floor width-to-height ratios (*Vf*; 0.08–0.37), and hypsometric integral (*HI*; 0.31–1.05) suggest relatively higher tectonic activity along western and southern part of the basin. Hypsometric curves for all segments of the faults mostly exhibit concave or straight profiles, signifying existence of young mountain fronts in the Çameli Basin. These calculations indicate that the Çameli Basin is tectonically active and, southern/south-western areas of this depression have earthquake potential, consistent with epicentres of recent earthquakes, occurred along some fault segments. Possible reason of this activity seems to be related to the E–W-trending corridor lying between the Gulf of Gökova and south-eastern part of the Çameli Basin, represented by active normal faults. These findings should be valid beyond the Çameli Basin for similar situations along the Isparta Angle's western margin.

Keywords: Çameli Basin; geomorphic indices; seismic activity; Isparta Angle; Western Anatolia

1. Introduction

Active tectonism plays an important role in a region's surface dynamics, controlling the density, pattern and geometry of basins' drainage systems (Strahler, 1964). The interaction between tectonism and drainage network geometry creates quantitatively measurable morphological features that influence the relative tectonic activity of the fault segments controlling the basin's development (Bull, 1977; Bull & McFadden, 1977; Burbank & Anderson, 2001; Keller, 1986; Keller & Pinter, 2002; Rockwell, Keller, & Johnson, 1984). These features, including mountain-front sinuosity, drainage basin shape and river channel asymmetry, are reliable tools for analysing the tectonism in continental extensional areas (Bull, 1977; Bull & McFadden, 1977; Gürbüz & Gürer, 2008; Keller, 1986; Keller & Pinter, 2002; Özkaymak, 2014; Özkaymak & Sözbilir, 2012; Ramirez-Herrera, 1998; Silva, Goy, Zazo, & Bardají, 2003; Wells et al., 1988; Yıldırım, 2014).

By the end of 1970s, numerical-based active tectonic measurements have been subjected to many studies worldwide. But in Western Anatolia, these kinds of geomorphological studies are very rare to measure the amount of tectonic activity in the region except Stewart and Hancock (1988); Paton (1992); Westaway et al. (2003); Özkaymak and Sözbilir (2012); and Özkaymak (2014).

Western Anatolia has experienced NNW–SSE-oriented continental extension since the Early Miocene

(Bozkurt, 2001; Mart & Woodside, 1994; McKenzie, 1978; Meulenkamp, Wortel, Van Wamel, Spakman, & Hoogerduyn Strating, 1988; Özkaymak & Sözbilir, 2008; Papazachos & Comninakis, 1971; Şengör & Yılmaz, 1981; Uzel & Sözbilir, 2008 and references therein). This continental extension has created several fault-controlled basins located between the central and southern regions of Western Anatolia Extensional Province (WAEP; Figure 1).

The Çameli Basin is such an area located in the WAEP that is controlled by NE-trending seismically active faults. This study was conducted to evaluate the geomorphological features of the Çameli Basin using geomorphic indices and to assess the relative activity potentials of the fault segments in this depression. The presence of numerous touristic and mercantile areas, located around the Çameli Basin, increases the importance of this study. Besides, the basin is located on the Fethiye-Burdur Fault Zone, a controversial fault zone which constitutes western limb of the Isparta Angle. The results of the study will contribute to the understanding of this structure.

2. Geological setting

2.1. Western Anatolia

The southern to south-western movement of Western Anatolia onto the African plate along the Aegean–Cyprian subduction zone formed the WAEP, which is characterised
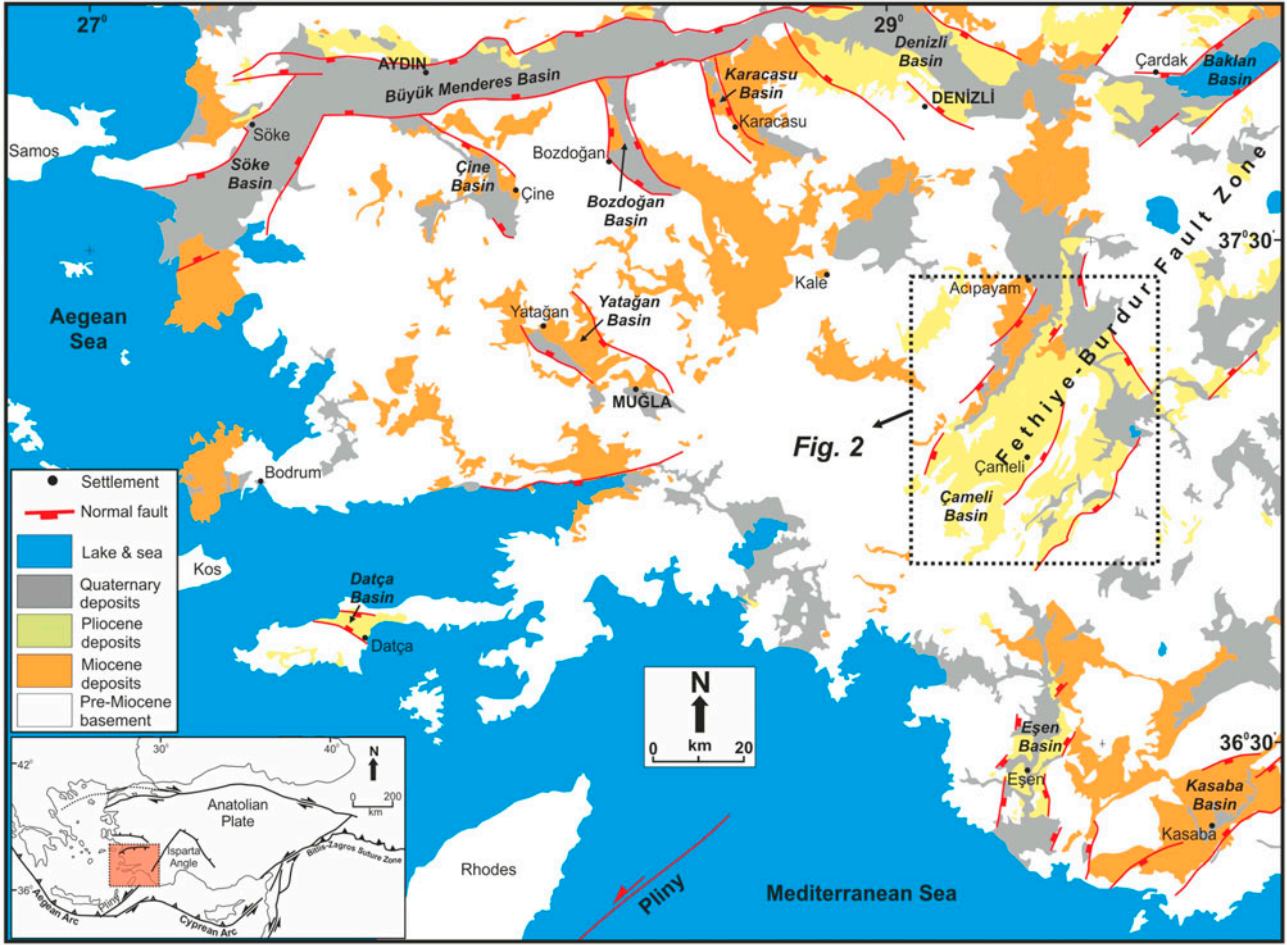

Figure 1. Simplified geological map of Western Turkey showing the major grabens (modified from Şenel, 2002).

by a NNW–SSE tensional stress regime (Mart & Woodside, 1994; McKenzie, 1978; Meulenkamp et al., 1988; Papazachos & Comninakis, 1971; Şengör & Yılmaz, 1981). This regime led to the formation of numerous intramontane basins in western and south-western Turkey (e.g. Şengör, Görür, & Şaroğlu, 1985; Şengör & Yılmaz, 1981): specifically, the Büyük Menderes, Çameli, Söke, Çine, Bozdoğan, Karacasu, Denizli, Baklan, Yatağan, Datça, Eşen, and Kasaba basins (Figure 1).

According to geodetic velocity measurements and structural and seismic studies, the WAEP is deformed by high strain rates characterised by dominantly E–W- and NE–SW-oriented normal faults (e.g. Barka & Reilinger, 1997; Doğru, Görgün, Özener, & Aktuğ, 2014; Kahle et al., 1998; Kurt, Demirbağ, & Kuşçu, 1999; Özener, Doğru, & Acar, 2013) and NE-trending dextral İzmir-Balıkesir Transfer Zone, firstly defined by Sözbilir, İnci, Erkül, and Sümer (2003), supported by several studies (e.g. Erkül, Helvacı, & Sözbilir, 2005; Ersoy, Helvacı, & Palmer, 2011; Özkaymak, Sözbilir, & Uzel, 2013; Uzel, Sözbilir, & Özkaymak, 2012). Another important structure located in the WAEP is the Fethiye-Burdur Fault Zone, firstly defined by Dumont, Poisson, and Şahinci (1979). The characteristics of this wide zone are controversial.

First group of researchers suggest that the zone is sinistral strike-slip fault zone (transtensional) (e.g. Dumont et al., 1979; Elitez & Yaltırak, 2014; Elitez, Yaltırak, Hall, Aksu, & Çifçi, 2015; Hall, Aksu, Elitez, Yaltırak, & Çifçi, 2014; Price & Scott, 1994; Şaroğlu, Boray, & Emre, 1987; Taymaz, Jackson, & McKenzie, 1991; Taymaz & Price, 1992) and it is the continuation of Pliny-Strabo trench in the Anatolian plate constituting the eastern boundary of the WAEP (e.g. Barka & Reilinger, 1997; Dumont et al., 1979; Gürer, Bayrak, Gürer, & İlkışık, 2004). The second group claims that the zone is characterised by normal faulting due to continental extension in Western Anatolia (e.g. Alçiçek, 2015; Alçiçek, Kazancı, & Özkul, 2005; Alçiçek, ten Veen, & Özkul, 2006; Koçyiğit, Ünay, & Saraç, 2000; Over et al., 2010), while third one suggests multiple mechanism of deformation phases (e.g. Ten Veen, Boulton, & Alçiçek, 2009).

These normal faults and shear zones generate high frequency seismicity in the region. The 1933 Çivril (Denizli) (M: 5.7), 1939 Dikili (İzmir) (M: 6.6), 1941 Muğla (M: 6.0), 1949 Karaburun (İzmir) (M: 6.6), 1955 Söke (Aydın) (M: 6.8), and 1965 Denizli earthquakes (M: 5.7) represent the largest recorded events (earthquake magnitudes are obtained from www.koeri.boun.edu.tr),

and numerous devastating historical earthquakes have been documented in the region (e.g. Altunel, Stewart, Piccardi, & Barka, 2003; Ocakoğlu et al., 2013).

2.2. Çameli Basin

The Çameli Basin is a key depression in Western Anatolia. The NE-trending basin is located between the Büyük Menderes Basin to the north and the Aegean Arc to the south and is approximately 60 km long and 40 km wide. Its northern margin has steep topography, with elevations between 700 and 2419 m (Mt. Gölgelidağ), while the southern area has an elevation of approximately 1700 m. The Dalaman River constitutes the main drainage for the basin, and Gölhisar Lake is the area's main water body (Figure 2).

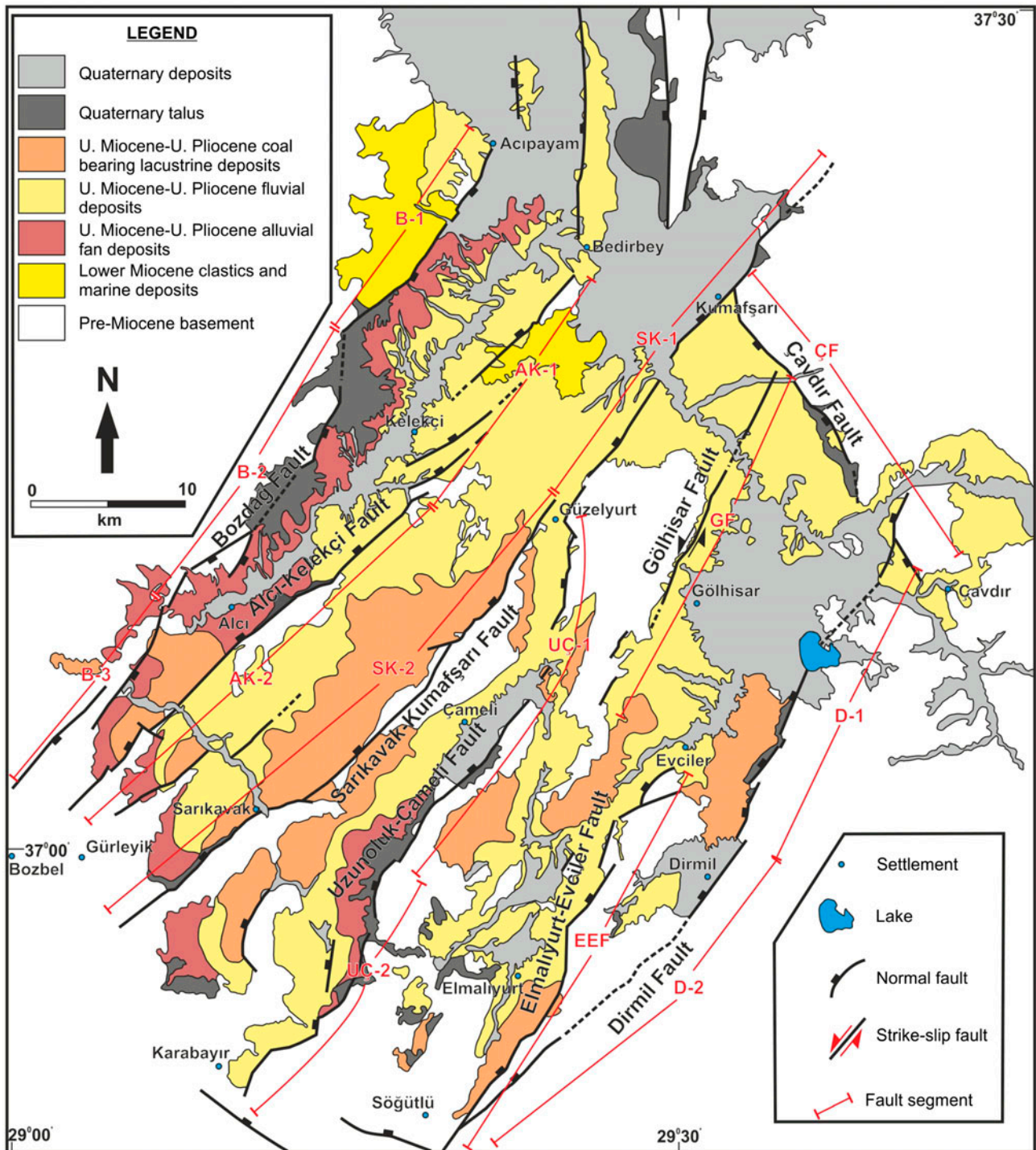The oldest basin deposits are Lower Miocene clastics consisting of conglomerates, sandstones, and mudstones

Figure 2. Simplified geological map of the Çameli Basin (from Alçiçek et al., 2005) showing the segmentation of the fault zones.

(Alçiçek et al., 2005, 2006), which unconformably over-lie dominantly Lower Cretaceous peridodites of the Lycian nappes (e.g. De Graciansky, 1972; Seyitoğlu, Işık, & Çemen, 2004) and Jurassic-Cretaceous neritic limestones of the Beydağları platform carbonates (e.g. Poisson, Yağmurlu, Bozcu, & Şentürk, 2003). These clastics grade to marine deposits composing of marl and reefal limestones of the same age. Upper Miocene–Upper Pliocene terrestrials cover these units unconformably, initially with conglomerates-sandstone-mudstone alternation followed by travertine and coal deposits, while lacustrine units constitute the top of this sequence (Alçiçek et al., 2005). Quaternary alluvium, an alluvial fan, talus, and recent lacustrine sediments are the basin's youngest deposits (Alçiçek, 2010; Alçiçek et al., 2005, 2006; Atalay, 1980; Becker-Platen, 1971).

Alçiçek et al. (2005) and Alçiçek and ten Veen (2008) have defined eight major fault zones for the Çameli Basin. The NE-trending Bozdağ and Dirmil Faults, characterised by SE- and NW-dipping normal faults respectively and the juxtaposition of basement rocks with basin deposits, constitute the boundaries of the basin (Figure 2). The Bozdağ Fault is approximately 55 km long and lies between Acıpayam to the NE and Bozbel to the SW. This fault consists three segments (B-1, B-2 and B-3; Figure 2) and named as 'Acıpayam Fault' in Active Fault Map of Turkey (Emre, Duman, Özalp, & Elmacı, 2011). All the segments are referred as active faults and represented as normal faults with sinistral strike-slip component. Commonly, the NW-trending Çavdır Fault (ÇF in this study) is also a boundary fault represented by SW-dipping normal faults extending between Kumafşarı and Çavdır with a length of approximately 20 km. The Dirmil Fault bounds the basin from SE and lies between Söğütlü to the SW and Çavdır to the NE. It is approximately 50 km long and characterised by NW-dipping fault planes. The Alçı-Kelekçi, Sarıkavak-Kumafşarı, Uzunoluk-Çameli, and Elmalıyurt-Evciler fault zones are intrabasinal normal faults generated by NW–SE-oriented progressive extension. The Alçı-Kelekçi Fault is approximately 50 km long and located between Bedirbey to the NE and Bozbel to the SW. It is characterised by NW-dipping normal faults and evaluated in two segments, namely AK-1 and AK-2, in this study (Figure 2). The AK-2 segment of the fault is referred as active (namely 'Kelekçi Fault') by Emre et al. (2011) and presented as pure normal fault. The Sarıkavak-Kumafşarı Fault, located between Gürleyik to the SW and Kumafşarı to the NE, is about 65 km long and composed of two fault segments having NW-dipping fault planes, namely SK-1 and SK-2 (Figure 2). SK-1 segment is represented as probable NW-dipping active fault by Emre et al. (2011). The Uzunoluk-Çameli Fault is about 45 km long normal fault, characterised by NW-dipping fault planes. This fault is also evaluated in two segments, namely UÇ-1 and UÇ-2. It lies between Karabayır t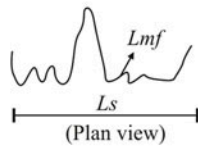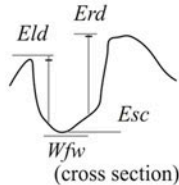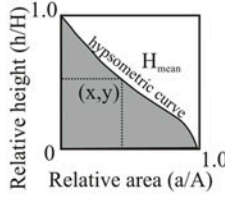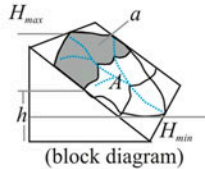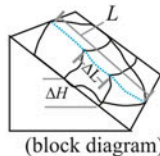o the SW and Güzelyurt to the NE (Figure 2). The UÇ-1 segment is represented with sinistral active Quaternary fault and named as 'Çameli Fault' by Emre et al. (2011). The Elmalıyurt-Evciler Fault (EEF) is situated at the south-western part of the basin between Söğütlü to the SW and Evciler to the NE. It is approximately 30 km long and denoted by NW-dipping fault planes. The Gölhisar Fault (GF) has the same trend as the boundary faults and is the only strike-slip (sinistral) fault observed in the study area (Figure 2). It is located between SW of Gölhisar and NE of Çavdır with a length of approximately 25 km. Although being represented as strike-slip, this fault is also evaluated with others due to the possibility of being a reactivated fault which may formerly formed as a normal fault.

Alçiçek and ten Veen (2008) indicate that the basin initially formed as a piggy-back basin and experienced three pulses during the rifting period (Alçiçek et al., 2005). The first tectonic pulse was related to the initiation of the Çameli Basin during the Late Miocene, while the second (Early–Middle Pliocene) and third (Latest Pliocene) pulses expanded the basin and created progressively inward development of the depression (Alçiçek et al., 2005). Recent kinematic studies indicate that the basin's stress field falls into two stages: NW–SE-oriented extension, related to the southward retreat of the slab, which has prevailed since the Plio-Quaternary, followed by N–S-oriented extension associated with the combined Anatolian extrusion and subduction processes (Over et al., 2010).

3. Methods

Digitised 1:25000-scale topographic maps were used to calculate geomorphic indices for the Çameli Basin. The stream network and related calculations were computed with ArcGIS (ver. 10.2) and the TecDEM toolbox using Matlab™ (ver. 2014b). A simplified geological map of the study area (from Alçiçek et al., [2005]) was used to determine the rock strength. The previous nomenclature for the fault zones was preserved, and 14 segments of eight fault zones in the Çameli Basin were evaluated separately, according to their position and step-over zones in the depression (Figure 2). The geomorphic indices used in this study included the hypsometric curve, the hypsometric integral, the mountain-front sinuosity, the ratio of the valley floor width to the valley height, and the stream length–gradient index (Table 1). Selby's (1980) classification was used in this study for classification of rock strength. According to this classification, the peridodites and limestones of the basement rocks are attributed to very high strength, Miocene continental clastics are classified as having high strength, Miocene lacustrine deposits are classified as having moderate strength, Pliocene terrestrial clastics are classified as having low strength, and recent alluvial deposits are classified as having very low strength according to their resistance to erosion.

Table 1. Summary of the morphometric parameters used in this study (modified from Keller & Pinter, 2002; Özkaymak, 2014).

Morphometric parameter	Mathematical derivation[a]	Measurement procedure	Explanation	Source
Smf, Mountain front sinuosity	$Smf = Lmf/Ls$	(Plan view)	Reflect a balance between the tendency of stream and slope processes to produce irregular (sinuous) mountain front and vertical active tectonics that tend to produce a prominent straight front. Smf >1.4–most tectonic activity; Smf >1.4–less tectonic activity	(1, 2, 3, 4, 5, 6)
Vf, valley floor width-to height ratio	$Vf = 2Vfw/[(Eld - Esc) + (Erd - Esc)]$	(cross section)	Define the ratio of the width of the valley floor to the mean height of two adjacent divides. The index reflects differences between broadfloored canyons with relatively high values of Vf, and V-shaped canyons with relatively low Vf values	(2, 3, 4)
Hypsometric curve	$x = a/A$ $y = h/H$		Describes the distribution of elevations across an area of land. Convex hypsometric curves characterise relatively 'young' weakly eroded regions, S-shaped curves characterise moderately eroded regions, and concave curves characterise relatively 'old' highly eroded regions	(3)
HI, Hypsometric integral	$HI = (h_{mean} - h_{min})/(h_{max} - h_{min})$	(block diagram)	Known as basin-area altitude distrubution and defined as the area under the hypsometric curve. Higher values of HI indicate that most of the topography is high relative to the mean. Intermediate (straight or S-shaped curves) to low (upwardly concave curves) values are associated with more evenly dissected drainage basins	(3)
SL, Stream length-gradient index	$SL = (\Delta H/\Delta L) \cdot L$	(block diagram)	Total or available stream power is related to the slope of the water channel. Sudden changes in SL values along the stream channel indicate lithological differences and/or possible tectonic activity	(3, 5, 7, 8)

Sources: (1) Bull (1977); (2) Bull and McFadden (1977); (3) Keller and Pinter (2002); (4) Silva et al. (2003); (5) El Hamdouni et al. (2008); (6) Rockwell et al. (1984); (7) Hack (1973); (8) Alipoor et al. (2011).
a Symbols: *Lmf* – length of mountain front along the mountain-piedmont junction; *Ls* – straight-line length of the front; *Vfw* – width of valley floor; *Eld* and *Erd* – respective elevations of the left and right valley divides; *Esc* – elevation of the valley floor; *x* and *y* – axes; *a* – surface area within the basin above a given line of elevation; *A* – total surface area of the basin; *h* – given line of elevation; *Hmean* – mean elevation; *Hmin* – minimum elevation; *Hmax* – maximum elevation; *ΔH* – change in elevation of the reach; *ΔL* – length of the reach; *L* – total channel length from the point of interest where the index is being calculated upstream to the highest point on the channel.

4. Results

4.1. Hypsometric curve and HI

Hypsometric curves were calculated for each drainage basins, which are controlled by fault segments in the Çameli Basin and indicate the presence of two groups of fault segments. Convex curvature, indicating relatively high tectonic activity, was obtained for B-1, AK-2, SK-1, GF, EEF, D-1. B-2, B-3, UÇ-1, D-2, and ÇF.

AK-1, SK-2 and UÇ-2 showed linear trends indicating lower activity. The HI values obtained, ranging from 0.31 to 1.05, suggest the presence of three groups of fault segments. Lower values, indicating low tectonic activity, were obtained for B-3, AK-1, EEF, GF, B-1, SK-1, and D-1. Moderate values were obtained for ÇF and B-2. The highest values were obtained for AK-2, SK-2, UÇ-1, UÇ-2, and D-2 (Figure 3 and Table 2).
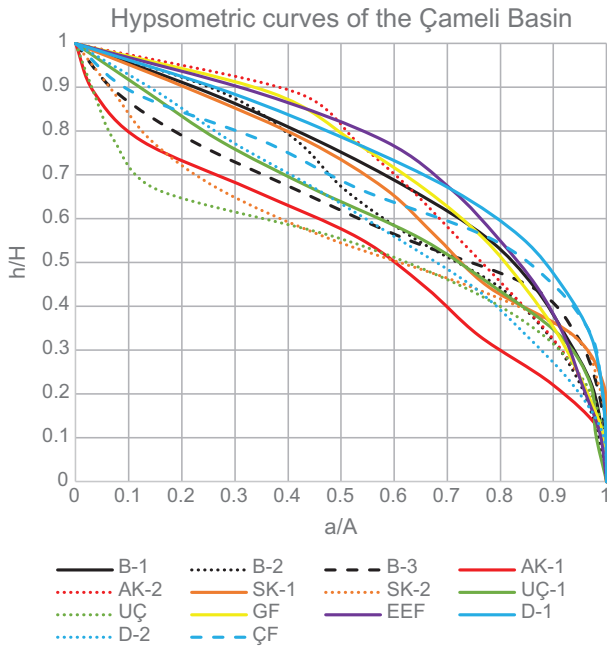
Figure 3. Hypsometric curves of the Çameli Basin's drainage system. The colours for different fault segments are indicated in the legend.

Table 2. Morphological properties of segments of the fault zones in the Çameli Basin, showing *HI* (hypsometric integral), *Smf* (mountain-front sinuosity ratio), and mean and standard deviation of *Vf* (valley floor width-to-height ratio).

Segment	*HI*	*Smf*	*Vf* (mean)	Standard deviation (*Vf*)
B-1	0.35	1.37	0.37	0.25
B-2	0.50	1.43	0.21	0.07
B-3	0.43	2.15	0.19	0.11
AK-1	0.42	1.50	0.31	0.12
AK-2	1.05	1.66	0.29	0.22
SK-1	0.32	1.48	0.08	0.05
SK-2	0.87	1.40	0.13	0.07
UÇ-1	1.03	1.71	0.23	0.10
UÇ-2	0.71	2.39	0.13	0.08
D-1	0.31	1.97	0.17	0.13
D-2	0.64	1.62	0.20	0.07
EEF	0.40	1.73	0.26	0.25
GF	0.35	1.35	0.19	0.15
ÇF	0.56	1.77	0.13	0.04

4.2. Mountain-front sinuosity (*Smf*)

The *Smf* values obtained for the Çameli Basin ranged from 1.35 to 2.39 (Figure 4 and Table 2). The GF and B-1 segments of the Bozdağ Fault had the lowest *Smf*
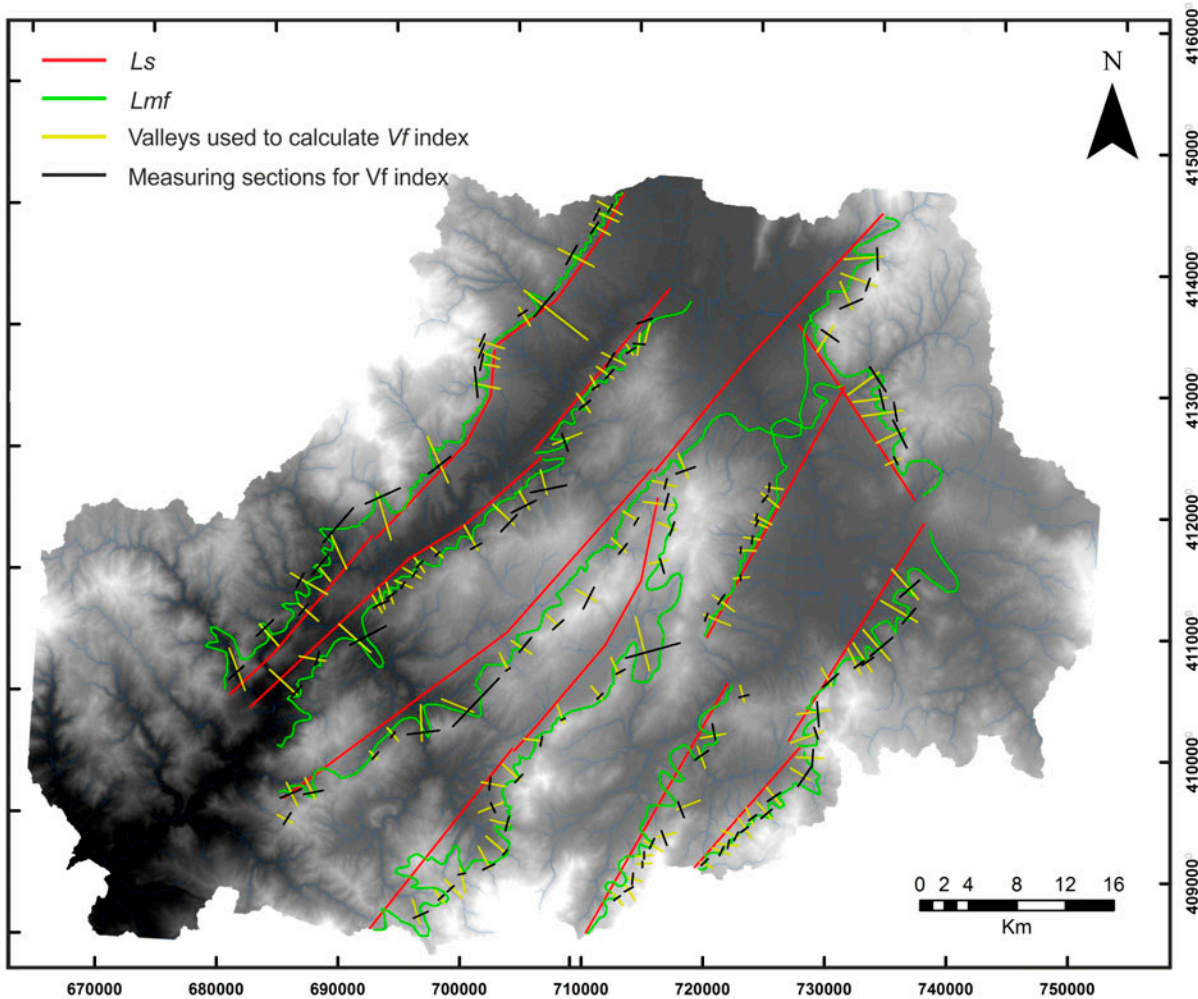

Figure 4. Schematic watershed map of the Çameli Basin showing the *Smf* (mountain-front sinuosity) and *Vf* (ratio of valley floor width to valley height index) lines used for the calculation in the study area.

values, indicating relatively active faults. The B-3 segment of the Bozdağ Fault (2.15) and the UÇ-2 segment of the Uzunoluk-Çameli Fault (2.39) had the highest values, indicating that they are relatively stable branches. The *Smf* values of the remaining fault segments ranged from 1.40 to 1.97.

4.3. Ratio of valley floor width to valley height index (Vf)

The mean *Vf* values obtained ranged from 0.13 to 0.37 (Figure 4 and Table 2). The lowest values were obtained for SK-1, SK-2, UÇ-2, D-1, and ÇF, indicating v-shaped valleys.
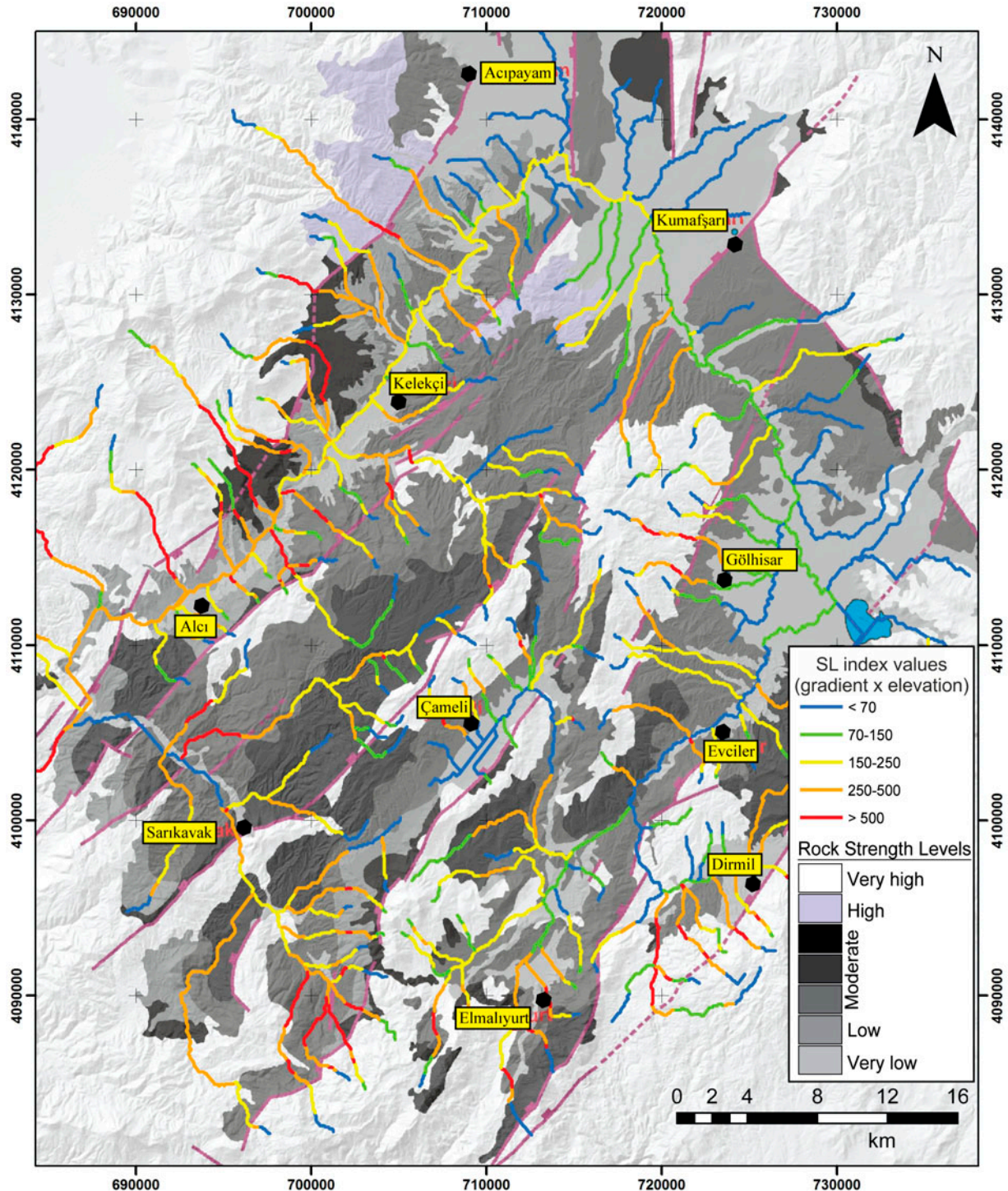

Figure 5. Simplified map showing the *SL* (stream length–gradient index) indices along the drainage paths of the Çameli Basin. Selby's (1980) rock strength classification was applied to study area's geological map.

4.4. Stream length–gradient index (SL)

The *SL* values for streams cutting through the fault segments ranged from 2.78 to 12,190. The lowest values were obtained for the Çameli Basin's main drainage region and the upstream reaches of the drainage basins. The highest values, related to faults rather than lithological changes, were obtained for B-1, B-2, B-3, AK-2, UÇ-2, D-2, and GF (Figure 5) and represent streams aligned with the faults' strikes.

5. Discussion

5.1. Interpretation of geomorphic indices and relative tectonic activity assessment of segments

The hypsometric curves of the fault segments indicate that the highest potential for tectonic activity should be expected in the central and southern parts of the basin (southwestern segments of the Alcı-Kelekçi, Sarıkavak-Kumafşarı, Uzunoluk-Çameli, and Dirmil faults), with relatively lower potential for tectonic activity in the northern and north-eastern parts of the basin (Bozdağ, Gölhisar and Çandır faults). The *HI* calculations mostly support the hypsometric curve data, with some differences that suggest relatively high activity for the Bozdağ, Gölhisar and Elmalıyurt-Evciler fault segments. The *HI* values indicating higher tectonic activity is compatible with those obtained from the Honaz Fault ($0.73 > HI > 0.61$) (Özkaymak, 2014) or the Spildağı ($HI > 0.61$) (Özkaymak & Sözbilir, 2012) located to the north and north-west of the study area, respectively.

The smallest *Smf* values obtained corresponded to B-1, B-2, SK-2, and GF, indicating relatively high tectonic activity, followed by AK-1, SK-1, and D-2. A third group had lower values that still demonstrated high potential for tectonic activity, in contrast to values obtained in similar study of the Tuz Gölü Fault Zone in Central Anatolia (*Smf*: 1.5–2.3) (Yıldırım, 2014). The Honaz Fault (*Smf*: 1.14) (Özkaymak, 2014) or the Spildağı (*Smf*: 1.11–1.14) (Özkaymak & Sözbilir, 2012) in Western Anatolia shows lower *Smf* values corresponding to higher tectonic activity and related uplift rates compared to those obtained in the study area. This difference can be related to the transtensional characteristics of the Fethiye-Burdur Fault Zone suggested by Barka and Reilinger (1997) which can reduce uplift rates of the region.

The *Vf* and *Smf* index values obtained were similar for SK-1, SK-2, UÇ-2, D-1, GF, and ÇF, with the lowest values indicating high activity. The *Vf* values were also found to be correlated to the *Smf* values, which made it possible to estimate the activity class and uplift rate for each segment (Figure 6). As this figure shows, B-1, B-2, SK-1, SK-2, AK-1, and GF exhibit high activity, with uplift rates > 0.5 mm/yr, while the remaining segments exhibit moderate activity, with uplift rates between 0.05 and 0.5 mm/yr. These uplift rates are consistent with Middle to Late Pliocene rates (0.2–0.3 mm/yr) that have been suggested for the Western Anatolian Province (Demir, Yeşilnacar, & Westaway, 2004) and Pliocene to Quaternary rates (0.1–0.2 mm/yr) that have been
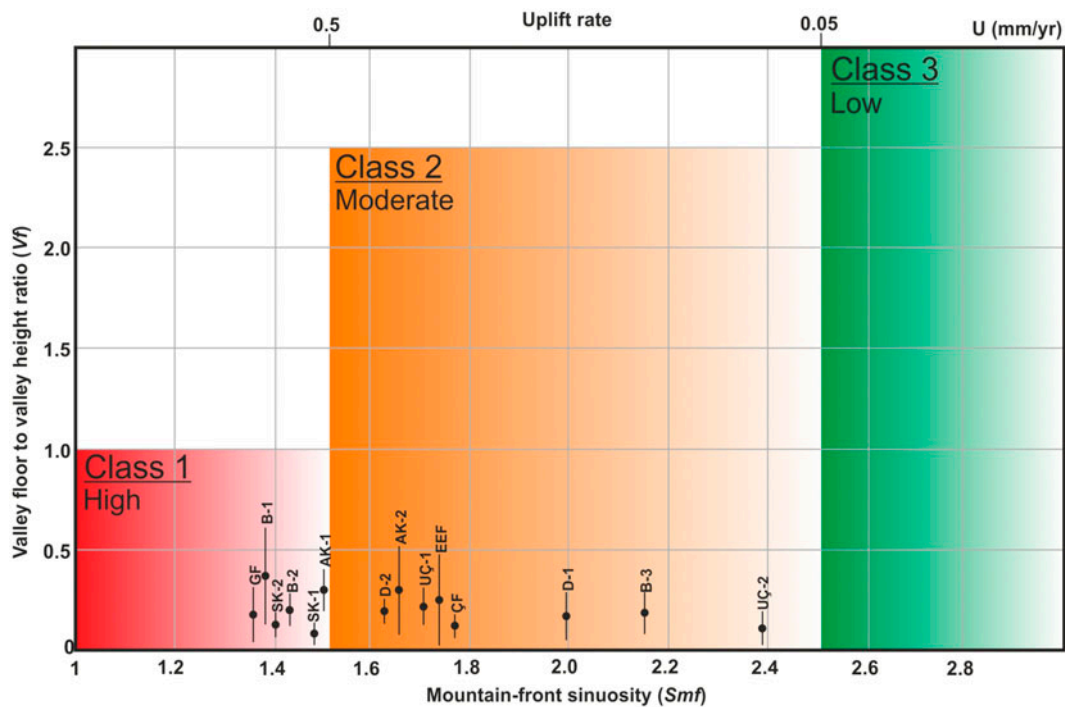

Figure 6. Chart showing the *Smf* vs. *Vf* values (vertical bars show standard deviations for *Vf* values) for the mountain fronts of the Çameli Basin and inferred activity classes (Silva et al., 2003). The upper *x*-axis indicates inferred uplift rates *U* (mm/yr) (from Rockwell et al., 1984; Yıldırım, 2014).

suggested for the Büyük Menderes region (Westaway et al., 2003). Within this manner, the GF may formerly formed as an intrabasinal fault and later acted as sinistral strike-slip fault. This situation can explain the lower *Smf* and *Vf* values calculated for the GF.

The *SL* values obtained are also consistent with the results obtained for other geomorphic indices. The higher *SL* values obtained for B-1, B-2, and B-3 are consistent with higher activity in the northern margin of the Çameli Basin. Additionally, GF (the only strike–slip fault in the basin), the south-western segments of the central fault zones, and the basin's southern marginal segment all exhibit activity similar to that observed at the northern margin. The values gradually increase uphill, indicating rock strength changes due to the juxtaposition of basement units and basin deposits. In all fault segments, higher values along the stream channels are obtained from the fault scarps where dominantly basement and basinal deposits juxtapose (B-1, B-2, B-3, UÇ-2, SK-2, GF, and D-2) and, along the channels of different intabasinal deposits juxtaposing by the faults (AK-1 and AK-2).

The results discussed above for the geomorphic indices considered indicate that the highest tectonic activity can be expected in the B-1 and B-2 segments of the Bozdağ Fault, both two segments of the Alcı-Kelekçi Fault, the Gölhisar Fault, the Sarıkavak-Kumafşarı Fault and UÇ-1 segment of the Uzunoluk-Çameli Fault. These results are mostly compatible with the active/potentially active faults (Acıpayam, Kelekçi, and Çameli faults) suggested by Emre et al. (2011). High to moderate activity can be expected for the D-2 segment of the Dirmil Fault and the Elmalıyurt-Evciler Fault. The remaining segments exhibit low to moderate activity. No segments exhibited low tectonic activity or stable conditions.

5.2. Regional impact of the results and implications for seismic hazards

The Western Anatolia is the most seismically active region of Turkey. The distribution of the earthquake epicentres having magnitude ≥ 4.5 are mostly located around Gulf of Gökova, Pliny trench and NE- and NW-trending corridors located to the north of the Çameli Basin (Figure 7, Table 3). In the Gulf of Gökova region, focal mechanism solutions of the recent earthquakes show that the seismic activity is observed along E–W-trending normal faults due to N–S-oriented extension. The solutions located at the southern part of the Çameli Basin is quite compatible with those in the Gökova
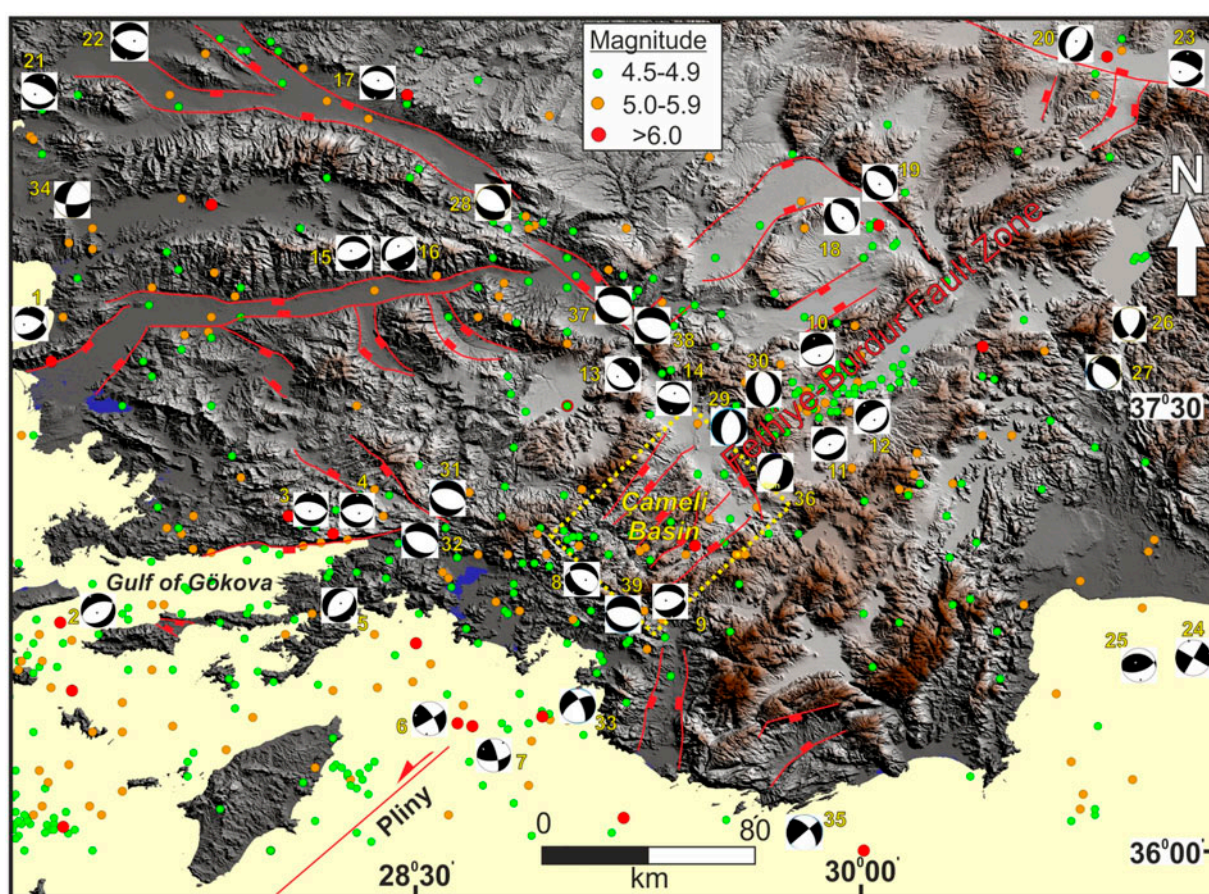
Figure 7. Digital elevation model showing the epicentres of earthquakes with magnitudes ≥ 4.5 that occurred in southwestern Anatolia between 1901 and 2015 (the earthquake data were taken from www.koeri.boun.edu.tr). Yellow numbers indicate the focal mechanism solutions of the earthquakes (see Table 3 for earthquake information; compiled from Barka, Reilinger, Şaroğlu, & Şengör, 1997; Emre et al., 2011; Koçyiğit, 2000; Tan, Tapırdamaz, & Yörük, 2008).

Table 3.   Information about the earthquakes having magnitude ≥ 4.5 occurred in western and south-western part of Turkey (compiled from Jackson & McKenzie, 1984; McKenzie, 1972, 1978; Tan et al., 2008; Taymaz, 1993; Taymaz, Tan, & Yolsal, 2004; EMSC 'Euro-Med seismological centre').

Earthquake No	Date (dd mm yyyy)	Latitude (°)	Longitude (°)	Magnitude	Focal depth (km)
1	16 07 1955	37.60	27.20	6.8	–
2	04 08 2004	36.84	27.78	5.2	10
3	27 04 1989	37.04	28.17	5.3	12
4	28 04 1989	37.03	28.11	5.1	17
5	05 10 1999	36.75	28.24	4.8	17
6	24 04 1957	36.37	28.59	6.9	48
7	25 04 1957	36.47	28.56	7.1	53
8	13 11 1994	36.92	29.05	4.9	10
9	18 07 1990	37.00	29.57	5.1	26
10	12 05 1971	37.64	29.72	5.5	30
11	12 05 1971	37.60	29.68	5.3	36
12	12 05 1971	37.58	29.60	5.3	33
13	21 04 2000	37.88	29.36	4.8	20
14	13 06 1965	37.85	29.32	5.1	33
15	11 10 1986	37.94	28.56	5.4	5
16	25 04 1959	37.97	28.50	6.1	–
17	28 03 1969	38.55	28.46	5.9	4
18	04 04 1998	38.10	30.15	4.9	19
19	01 10 1995	38.06	30.15	5.8	5
20	03 02 2002	38.63	30.88	5.6	25
21	16 12 1977	38.41	27.19	5.3	24
22	28 01 1994	38.69	27.50	5.2	10
23	03 02 2002	38.52	31.20	5.6	22
24	01 06 1977	36.16	31.30	5.6	68
25	30 04 1975	36.19	30.74	5.6	61
26	10 04 2007	37.99	30.99	4.8	10
27	30 03 2007	37.99	30.96	4.7	10
28	23 01 2007	38.15	28.76	4.7	2
29	16 02 2015	37.21	30.00	4.8	10
30	16 08 2008	37.33	29.96	4.5	5
31	10 11 2014	37.14	28.78	4.7	13
32	16 05 2013	37.05	28.39	4.8	3
33	25 06 2012	36.39	29.01	5.0	44
34	20 02 2012	38.15	27.47	4.5	7
35	14 10 2010	36.10	29.61	4.6	30
36	04 12 2009	37.38	29.65	4.8	15
37	04 12 2009	37.91	28.83	5.2	10
38	25 04 2008	37.83	29.32	4.8	10
39	29 10 2007	36.96	29.29	5.2	20

region, presenting NE–SW- and N–S-oriented extension characterised by normal faults. But at Pliny trench, the solutions represent strike-slip faulting, matching with the characteristics of the zone. At the north-eastern part of the Çameli Basin, domination of NW–SE-oriented extension takes place on NE-trending normal faults (along the Fethiye-Burdur Fault Zone) while NW-trending corridor is represented by NW-trending normal faults with minor strike-slip component demonstrating NE-SW extension. At the junction of these corridors, E-W-oriented extension come front with almost N-S trending normal faults. At the northern part of the Gulf of Gökova, the Gediz, Büyük Menderes and Söke grabens show seismic activity compatible with the normal faults constituting the boundaries of these depressions. The single strike-slip dominated solution is thought to represent the seismicity of the İzmir-Balıkesir Transfer Zone.

The distribution of the earthquakes located around the Çameli Basin clearly shows that southern part of the basin has higher seismicity (Figure 7), matching with the results of this study. These earthquakes located at the southern part are represented by E–W-trending faults and are suggested as the continuation of the normal faults determined in the Gulf of Gökova (Elitez & Yaltırak, 2014; Hall et al., 2014). Although the orientation of these faults are different from those located in the study area, NE-trending and juxtaposing fault segments of the Çameli Basin can be affected by this seismicity.

The stream channels which cut the fault segments of the Çameli Basin do not represent uniform offsetting along the channels (see Figures 4 and 5 for the drainage pattern). This situation may be the consequence of the faults being normal character (Alçiçek, 2015; Alçiçek et al., 2005, 2006; Koçyiğit et al., 2000; Over et al.,

southwestern Anatolia, Turkey. *Sedimentary Geology, 173*, 409–431.

Alçiçek, M. C., ten Veen, J. H., & Özkul, M. (2006). Neotectonic development of the Çameli Basin, southwestern Anatolia, Turkey. In A. H. F. Robertson & D. Mountrakis (Eds.), *Tectonic development of the Eastern Mediterranean region* (pp. 591–611). Geological Society of London. London-UK Special Publication No. 260.

Alçiçek, M. C., & ten Veen, J. H. (2008). The late early Miocene Acıpayam piggy-back basin: Refining the last stages of Lycian nappe emplacement in SW Turkey. *Sedimentary Geology, 208*, 101–113.

Alipoor, R., Poorkermani, M., Zare, M., & El Hamdouni, R. (2011). Active tectonic assessment around Rudbar Lorestan damsite, high Zagros belt (SW of Iran). *Geomorphology, 128*(1–2), 1–14.

Altunel, E., Stewart, I. S., Piccardi, L., & Barka, A. (2003). Earthquake faulting at ancient Cnidus, SW Turkey. *Turkish Journal of Earth Sciences, 12*, 137–152.

Atalay, Z. (1980). Stratigraphy of continental Neogene in the region of Muğla-Yatağan. *Turkey Bulletin of Geological Society, C23*, 93–99 (in Turkish with English abstract).

Barka, A. A., & Reilinger, R. (1997). Active tectonics of the Mediterranean region: Deduced from GPS, neotectonic and seismic data. *Annali di Geofisica, XI*, 587–610.

Barka, A. A., Reilinger, R., Şaroğlu, F., & Şengör, A. M. C. (1997). The Isparta Angle: its importance in the neotectonics of the eastern Mediterranean region. In O. Pişkin, M. Ergün, M. Y. Savaşçın, G. Tarcan (Eds.), *International earth sciences colloquium on the aegean region* (Vol. 1, pp. 3–18), 9–14 October, 1995 İzmir-Göllük, Turkey.

Becker-Platen, J. D. (1971). Stratigraphic division of the neogene and oldest pleistocene in southwest Anatolia. *Newsletters on Stratigraphy, 1–3*, 19–22.

Bozkurt, E. (2001). Neotectonics of Turkey – A synthesis. *Geodinamica Acta, 14*, 3–30.

Bull, W. B. (1977). *Tectonic geomorphology of the Mojave Desert, California* (188 pp). US Geological Survey Contract Report 14-0-001-G-394. Menlo Park, CA: Office of Earthquakes, Volcanoes, and Engineering.

Bull, W. B., & McFadden, L. D. (1977). Tectonic geomorphology north and south of the Garlock fault, California. In D. O. Doehering (Ed.), *Geomorphology in arid regions. Proceedings of the eighth annual geomorphology symposium* (pp. 115–138). Binghamton, NY State University of New York.

Burbank, D. W., & Anderson, R. S. (2001). *Tectonic geomorphology.* Malden, MA: Blackwell Science.

Demir, T., Yeşilnacar, İ., & Westaway, R. (2004). River terrace sequences in Turkey: Sources of evidence for lateral variations in regional uplift. *Proceedings of the Geologists' Association, 115*, 289–311.

Doğru, A., Görgün, E., Özener, H., & Aktuğ, B. (2014). Geodetic and seismological investigation of crustal deformation near Izmir (Western Anatolia). *Journal of Asian Earth Sciences, 82*, 21–31.

Dumont, J. F., Poisson, A., & Şahinci, A. (1979). On the existence of recent sinistral sliding movements at the eastern end of the Aegean arc (south-eastern Turkey)[Sur L'existence de coulissements senestres récents a l'extrémité orientale de le arc Egeen (sud-ouest de la Turquie)]. C.R. Acad. Sc. Paris, 289, 261–264.

El Hamdouni, R., Irigaray, C., Fernández, T., Chacón, J., & Keller, E. A. (2008). Assessment of relative active tectonics, southwest border of the Sierra Nevada (southern Spain). *Geomorphology, 96*, 150–173.

Emre, Ö., Duman, T.Y., Özalp, S., & Elmacı, H. (2011). *1:250.000 scale active fault map series of Turkey, Denizli (NJ 35-12) quadrangle*. Serial number: 12. Ankara: General Directorate of Mineral Research and Exploration.

2010). Another option is the faults of the Çameli Basin's being generated in transtensional shear zone (Elitez & Yaltırak, 2014; Elitez et al., 2015; Hall et al., 2014) where the strain is distributed over many faults, consequently do not represent along-strike offsetting especially, along Quaternary strata (Elitez et al., 2015).

6. Conclusions

In this study, four geomorphic indices were applied to the Çameli Basin in south-western Anatolia. The analysis results clearly indicate that:

- The Bozdağ (the northwestern boundary of the basin), Alcı-Kelekçi, Sarıkavak-Kumafşarı, Uzunoluk-Çameli and Gölhisar faults exhibit higher tectonic activity than the northern and eastern segments.
- The Bozdağ, Sarıkavak-Kumafşarı, Alcı-Kelekçi, and Gölhisar faults represent higher uplift rates (>0.5 mm/yr) while remaining ones show lower (0.05–0.5 mm/yr). These results are well-matched with the previous studies carried out in other regions of western Anatolia.
- The fault segments representing higher tectonic activity are also mapped as active faults with different nomenclature in the Active Tectonic Map of Turkey (Emre et al., 2011) and are compatible with each other. None of the segments in the Çameli Basin show low tectonic activity or stable conditions.
- The reason of the faults' demonstrating relatively higher tectonic activity (mentioned above) can be related to the E–W-trending corridor lying between the Gulf of Gökova and the south-east of the Çameli Basin as they juxtapose.

Acknowledgements

References

Alçiçek, H. (2010). Stratigraphic correlation of the Neogene basins in southwestern Anatolia: Regional palaeogeographical, palaeoclimatic and tectonic implications. *Palaeogeo, 3*, 297–318.

Alçiçek, M. C. (2015). Comment on "The Fethiye–Burdur fault zone: A component of upper plate extension of the subduction transform edge propagator fault linking hellenic and cyprus arcs, eastern mediterranean. *Tectonophysics, 635*, 80–99" by J. Hall, A.E. Aksu, İ. Elitez, C. Yaltırak, G. Çiftçi. *Tectonophysics in press*. doi:10.1016/j.tecto.2015.01.025

Alçiçek, M. C., Kazancı, N., & Özkul, M. (2005). Multiple rifting pulses and sedimentation pattern in the Çameli Basin,

Elitez, İ., & Yaltırak, C. (2014). Miocene-quaternary geody-namics of Çameli Basin, Burdur–Fethiye shear zone (SW Turkey). *Geological Bulletin of Turkey, 57*, 41–67.

Elitez, İ., Yaltırak, C., Hall, J., Aksu, A. E., & Çifçi, G. (2015). Reply to the comment by M.C. Alçiçek on "The Fethiye–Burdur fault zone: A component of upper plate extension of the subduction transform edge propagator fault linking hellenic and cyprus, arcs Eastern Mediterranean," *Tectonophysics, 635*, 80–99, by J. Hall, A. E. Aksu, İ. Elitez, C. Yaltirak, & G. Çifçi. *Tectonophysics. in press.* doi:10.1016/j.tecto.2015.04.002

Erkül, F., Helvacı, C., & Sözbilir, H. (2005). Evidence for two episodes of volcanism in the Bigadiç borate basin and tec-tonic implications for western Turkey. *Geological Journal, 40*, 1–26.

Ersoy, E. Y., Helvacı, C., & Palmer, M. R. (2011). Stratigraphic, structural and geochemical features of the NE–SW-trending neogene volcano-sedimentary basins in Western Anatolia: implications for associations of suprade-tachment and transtensional strike-slip basin formation in extensional tectonic setting. *Journal of Asian Earth Science, 41*, 159–183.

De Graciansky, P. C. (1972). Geological research at the Wes-tern Lycian Taurus [Recherches geologiques dans le Taurus Lycien Occidental] (PhD Thesis). Paris-Sud University, Faculty of Sciences, Centre d'Orsay 896, Paris, France.

Gürbüz, A., & Gürer, Ö. F. (2008). Tectonic geomorphology of the North Anatolian fault zone in the lake Sapanca Basin (eastern Marmara Region, Turkey). *Geosciences Journal, 12*, 215–225.

Gürer, A., Bayrak, M., Gürer, F. Ö., & İlkışık, M. O. (2004). The deep resistivity structure of southwestern Turkey: Tectonic implications. *International Geology Review, 46*, 655–670.

Hack, J. T. (1973). Stream-profile analysis and stream-gradient index. *Journal of Research of the U. S. Geological Survey, 1*, 421–429.

Hall, J., Aksu, A. E., Elitez, I., Yaltırak, C., & Çifçi, G. (2014). The Fethiye–Burdur fault zone: A component of upper plate extension of the subduction transform edge propagator fault linking Hellenic and Cyprus Arcs, Eastern Mediterranean. *Tectonophysics, 635*, 80–99.

Jackson, J., & McKenzie, D. (1984). Active tectonics of the Alpine-Himalayan Belt between western Turkey and Pakistan. *Geophysical Journal of Royal Astronomical Society, 77*, 185–264.

Kahle, H. G., Straub, C., Reilinger, R., McClusky, S., King, R., Hurst, K., … Cross, P. (1998). The strain rate field in the Eastern Mediterranean region, estimated by repeated GPS measurements. *Tectonophysics, 294*, 237–252.

Keller, E. A. (1986). Investigation of active tectonics: Use of surficial earth processes. In R. E. Wallace (Ed.), *Active tec-tonics* (pp. 136–147). Washington, DC: National Academy Press. Studies in Geophysics.

Keller, E. A., & Pinter, N. (2002). *Active tectonics: Earth-quakes, uplift, and landscape*. New Jersey, USA NJ: Pren-tice Hall.

Koçyiğit, A. (2000). Seismicity of southwest Turkey. In *BAD-SEM 2000-seismicity of the West Anatolia symposium (Batı Anadolu'nun Depremselliği Sempozyumu)* (30–39), 24–27 May 2000, İzmir.

Koçyiğit, A., Ünay, E., & Saraç, G. (2000). Episodic graben formation and extensional neotectonic regime in west cen-tral Anatolia and the Isparta Angle: A case study in the Akşehir-Afyon Graben, Turkey. In E. Bozkurt, J. A. Winchester, & J. D. A. Piper (Eds.), *Tectonics and magma-tism in Turkey and the surrounding area* (Vol. 173, pp. 405–421). İzmir, TURKEY: Geological Society London Special Publication.

Kurt, H., Demirbağ, E., & Kuşçu, İ. (1999). Investigation of the submarine active tectonism in the Gulf of Gökova, southwest Anatolia–southeast Aegean sea, by multi-channel seismic reflection data. *Tectonophysics, 305*, 477–496.

Mart, Y., & Woodside, J. (1994). Preface: Tectonics of the Eastern Mediterranean. *Tectonophysics, 234*, 1–3.

McKenzie, D. (1972). Active tectonics of the Mediterranean Region. *Geophysical Journal of Royal Astronomical Soci-ety, 30*, 109–185.

McKenzie, D. (1978). Active tectonics of the Alpine-Himala-yan belt: The Aegean sea and surrounding regions. *Geo-physical Journal International, 55*, 217–254.

Meulenkamp, J. E., Wortel, W. J. R., Van Wamel, W. A., Spakman, W., & Hoogerduyn Strating, E. (1988). On the Hellenic subduction zone and geodynamic evolution of Crete in the late middle Miocene. *Tectonophysics, 146*, 203–215.

Ocakoğlu, F., Açıkalın, S., Güneş, G., Özkes, S., Dirik, K., & Özsayın, E. (2013). Was the 1899 Menderes valley earth-quake a double earthquake? Historical and paleoseismologi-cal constraints. *Journal of Asian Earth Sciences, 67–68*, 187–198.

Over, S., Pinar, A., Ozden, S., Yilmaz, H., Unlugenc, U. C., & Kamaci, Z. (2010). Late cenozoic stress field in the Cameli Basin, SW Turkey. *Tectonophysics, 492*, 60–72.

Özener, H., Doğru, A., & Acar, M. (2013). Determination of the displacements along the Tuzla fault (Aegean region-Turkey): Preliminary results from GPS and precise leveling techniques. *Journal of Geodynamics, 67*, 13–20.

Özkaymak, Ç. (2014). Tectonic analysis of the Honaz fault (western Anatolia) using geomorphic indices and the regio-nal implications. *Geodinamica Acta,.* Geodinamica Acta, 27:2-3, 110–129 Doi:10.1080/09853111.2014.957504.

Özkaymak, Ç., & Sözbilir, H. (2008). Stratigraphic and struc-tural evidence for fault reactivation: The active Manisa fault zone, Western Anatolia. *Turkish Journal of Earth Sciences, 17*, 615–635.

Özkaymak, Ç., & Sözbilir, H. (2012). Tectonic geomorphology of the Spildağı high ranges, Western Anatolia. *Geomor-phology, 173–174*, 128–140.

Özkaymak, Ç., Sözbilir, H., & Uzel, B. (2013). Neogene–Quaternary evolution of the manisa basin: Evidence for variation in the stress pattern of the Izmir–Balıkesir transfer zone, Western Anatolia. *Journal of Geodynamics, 65*, 117–135.

Papazachos, B. C., & Comninakis, P. E. (1971). Geophysical and tectonic features of the Aegean arc. *Journal of Geo-physical Research, 76*, 8517–8533.

Paton, S. (1992). Active normal faulting, drainage patterns and sedimentation in southwestern Turkey. *Journal of the Geo-logical Society of London, 149*, 1031–1044.

Poisson, A., Yağmurlu, F., Bozcu, M., & Şentürk, M. (2003). New data concerning the age of Aksu thrust in the south of the Aksu valley, Isparta Angle (SW Turkey): Concequences for the Antalya basin and the Eastern Mediterranean. *Geo-logical Journal, 38*, 311–327.

Price, S. P., & Scott, B. (1994). Fault block rotations at the edge of a zone of continental extension south–west Turkey. *Journal of Structural. Geology, 16*, 381–392.

Ramirez-Herrera, M. T. (1998). Geomorphic assessment of active tectonics in the Acambay graben, Mexican vol-canic belt. *Earth Surface Processes and Landforms, 23*, 317–332.

Rockwell, T. K., Keller, E. A., & Johnson, D. L. (1984). Tec-tonic geomorphology of alluvial fans and mountain fronts near Ventura, California. In M. Morisawa (Ed.), *Tectonic Geomorphology. Proceedings of the 15th annual geomor-phology symposium* (pp. 183–207). Boston, MA: Allen and Unwin.

Selby, M. J. (1980). A rock strength classification for geomorphic purposes: With tests from Antarctica and New Zealand. *Zeitschrift für Geomorphologie, 24*, 31–51.

Seyitoğlu, G., Işık, V., & Çemen, İ. (2004). Complete tertiary exhumation history of the Menderes massif, western Turkey: An alternative working hypothesis. *Terra Nova, 16*, 358–364.

Silva, P. G., Goy, J. L., Zazo, C., & Bardají, T. (2003). Fault-generated mountain fronts in southeast Spain: Geomorphologic assessment of tectonic and seismic activity. *Geomorphology, 50*, 203–225.

Sözbilir, H., İnci, U., Erkül, F., & Sümer, Ö. (2003). An active intermittent transform zone accommodating N-S extension in Western Anatolia and its relation to the North Anatolian fault system. International Workshop on the North Anatolian, East Anatolian and Dead Sea Fault Systems: Recent Progress in Tectonics and Paleoseismology, and Field Training Course in Paleoseismology, 31 August to 12 September 2003, Poster Session P:2/2, Ankara.

Stewart, I., & Hancock, P. (1988). Normal fault zone evolution and fault scarp degradation in the Aegean region. *Basin Research, 1*, 139–153.

Strahler, A. N. (1964). Quantitative geomorphology of drainage basins and channel networks. In Ven Te Chow (Ed.), International Association of Scientific Hydrology. Bulletin, 10:1, 82–83, DOI: 10.1080/02626666509493376.

Şaroğlu, F., Boray, A., & Emre, Ö. (1987). *Active faults of Turkey*. Ankara, TURKEY: Mineral Res. Explor. Inst. Unpublished report, 8643, 394 pp.

Şenel, M. (Ed.). (2002). *Türkiye Jeoloji Haritası [Geological map of Turkey] scale 1:500 000, 19 sheets*. Ankara: Maden Tetkik ve Arama Genel Müdürlüğü.

Şengör, A. M. C., & Yılmaz, Y. (1981). Tethyan evolution of Turkey: A plate tectonic approach. *Tectonophysics, 75*, 181–241.

Şengör, A. M. C., Görür, N., & Şaroğlu, F. (1985). Strike-slip faulting and related basin formation in zones of tectonic escape: Turkey as a key study. In K. T. Biddle & N. Christie-Blick (Eds.), *Strike-slip faulting and basin formation* (pp. 227–264). The Society of Economic Paleontologists and Mineralogists *Special Publication No. 37* Tulsa, Oklahoma-US ISBN: 0-918985-58-7.

Tan, O., Tapırdamaz, M. C., & Yörük, A. (2008). The earthquake catalogues for Turkey. *Turkish Journal of earth Sciences, 17*, 405–418.

Taymaz, T. (1993). The source parameters of Çubukdağ (W. Turkey) earthquake of 1986 October 11. *Geophysical Journal International, 113*, 260–267.

Taymaz, T., Jackson, J. A., & McKenzie, D. (1991). Active tectonics of the north and central Aegean Sea. *Geophysical Journal International, 106*, 433–490.

Taymaz, T., & Price, S. (1992). The 1971 May 12 Burdur earthquake sequence, SW Turkey: A synthesis of seismological and geological observations. *Geophysical Journal International, 108*, 589–603.

Taymaz, T., Tan, O., & Yolsal, S. (2004). Seismotectonics of western Turkey: A synthesis of source parameters and rupture histories of recent earthquakes. *AGU Fall Meeting, Session T14, San Francisco-California, EOS Transactions, 85*(47). Abstract T53B-0481

Ten Veen, J. H., Boulton, S. J., & Alçiçek, M. C. (2009). From palaeotectonics to neotectonics in the neotethys realm: The importance of kinematic decoupling and inherited structural grain in SW Anatolia (Turkey). *Tectonophysics, 473*, 261–281.

Uzel, B., & Sözbilir, H. (2008). A first record of a strike-slip basin in Western Anatolia and its tectonic implication: The Cumaovasi basin. *Turkish Journal of Earth Sciences, 17*, 559–591.

Uzel, B., Sözbilir, H., & Özkaymak, Ç. (2012). Neotectonic evolution of an actively growing superimposed basin in western Anatolia: The inner bay of Izmir, Turkey. *Turkish Journal of Earth Sciences, 22*, 439–471.

Wells, S. G., Bullard, T. F., Menges, C. M., Drake, P. G., Karas, P. A., Kelson, K. I., & Wesling, J. R. (1988). Regional variations in tectonic geomorphology along a segmented convergent plate boundary pacific coast of Costa Rica. *Geomorphology, 1*, 239–265.

Westaway, R., Pringle, M., Yurtmen, S., Demir, T., Bridgland, D., Rowbotham, G., & Maddy, D. (2003). Pliocene and quaternary surface uplift of western Turkey revealed by long-term river terrace sequences. *Current Science, 84*, 1090–1101.

Yıldırım, C. (2014). Relative tectonic activity assessment of the Tuz Gölü fault zone; Central Anatolia, Turkey. *Tectonophysics, 630*, 183–192.